

Synthesis, Crystal Structure, Spectroscopic Characterization and Anti-COVID-19 Molecular Docking Investigation of 2-(2-Formylphenoxy)acetamide

SELVARAJ GEETHA^{1,2,*}, RAJENDRAN SRIBALAN³ and SRINIVASAKANNAN LAKSHMI²

¹Department of Physics, Chevalier T. Thomas Elizabeth College for Women, Perambur, Chennai-600011, India

²Department of Physics, S.D.N.B. Vaishnav College for Women, Chromepet, Chennai-600044, India

³Biochemie Innovations Lab., Tindivanam-604001, India

*Corresponding author: E-mail: s.geetha15@gmail.com

Received: 29 June 2023;

Accepted: 3 August 2023;

Published online: 28 September 2023;

AJC-21388

Compound 2-(2-formylphenoxy)acetamide was synthesized by adopting the slow evaporation solution growth technique. The spectroscopic techniques were studied experimentally and theoretically at DFT for the title compound. The X-ray diffraction analysis confirmed its crystal structure. The compound with the molecular formula $C_9H_9NO_3$ crystallizes in the monoclinic crystal system with the centrosymmetric space group $P2_1/n$. The optimized structure, stability, hardness, softness, Mulliken charge distribution and molecular electrostatic potential (MEP) of the grown crystal were investigated using DFT calculations. Molecular docking studies were performed for the compound to evaluate its antiviral activity against SARS-CoV-2. The molecule has good binding affinity for the target protein 6NUS.

Keywords: 2-(2-Formylphenoxy)acetamide, Crystal structure, Molecular docking studies, DFT, Mulliken charge distribution.

INTRODUCTION

Planar rings of carbon atoms called heterocyclic compounds have at least one heteroatom like O, N, P or S in them [1,2]. Currently, many research chemists taking interest on the heterocyclic molecules that include nitrogen atom because nitrogen in heterocycle moiety exhibits the capability to readily absorb or donate a proton, in addition to its capacity to effortlessly form a wide range of weak interactions [3]. Based on the above knowledge, the research is focused on the synthesis and characterization of the amide functional group. Amides have a strong coordination property, which makes them frequently used as ligands [4,5]. Biological processes or molecular recognition events largely depend on the amide bond structure of amide derivatives [6]. The importance of the amide bond cannot be overstated because it forms the core of proteins, peptides and a wide range of other biomolecules essential to life. Biomolecules with a strong amide bond, which allows them to form more intra- and inter-hydrogen connections, can withstand chemically dangerous situations like an acidic or basic environment [7].

The resonance structure, which could form a double bond between carbon and nitrogen [8-10], is thought to be responsible

for the amide's exceptional stability. By making the molecule more planar and minimizing the free rotation of the carbon and nitrogen bonds, this resonance structure helped to create the three-dimensional (3D) structure of the biomolecules. The planar 3D structure of such compounds can interact with different biomolecules effectively, which may provide a solution to a variety of biological issues [11]. A wide range of amide-functionalized compounds have so far been described for a variety of biological activities [12]. Due to the structural resemblance between N-substituted 2-phenylacetamides and the lateral chain of natural benzylpenicillin, these molecules are extremely interesting [13,14]. Amides can be considered intrinsic substances from the biological perspectives, as they arise as a direct result of certain processes.

Knowing the significance of amides, in this work, an organic molecule containing an amide functional group was synthesized. The crystal structure of 2-(2-formylphenoxy)acetamide (FPA) was confirmed by single-crystal X-ray diffraction analysis and the molecule was analyzed by various spectroscopic techniques like Fourier transform infrared (FTIR), nuclear magnetic resonance (NMR), UV-visible and mass spectroscopy. A thorough study of the density functional theory (DFT) investigations

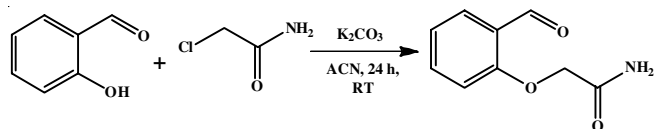
was also carried out in order to determine the molecules' activity and electronic structure. For 2-(2-formylphenoxy)acetamide, DFT has been used solely and/or in conjunction with experimental methods for understanding the bonding and structural properties, characterization and applications of the molecules.

Molecular docking helps to ascertain the interaction of molecules (ligands) with receptors and has been a useful technique in drug design and discovery. The molecule has a highly stable orientation in 3D view and is used for molecular docking experiments with a number of proteins that are involved in the SARS-CoV-2 infection. A pandemic of significant magnitude, spanning the previous three years, was caused by a unique single-stranded RNA virus belonging to the coronaviridae family. This global health crisis resulted in the slowdown of many societal activities over the entire globe [15,16]. Nevertheless, the establishment of COVID-19-free environments worldwide remains a formidable task, requiring the availability and widespread administration of effective pharmaceutical interventions.

Therefore, a new medication with a potent therapeutic agent must be discovered for COVID 19. When coronaviruses infect host cells, they form a multi-subunit RNA-synthesis complex comprising viral non-structural proteins (nsp), which are in charge of replicating and transcribing the viral genome. The 2-(2-formylphenoxy)acetamide molecule was investigated against SARS-CoV RNA polymerase proteins; of all proteins, 6NUS shows an acceptable binding energy and inhibition constant value. Protein 6NUS is SARS-CoV nsp12 polymerase bound to the nsp8 co-factor [17].

EXPERIMENTAL

Synthesis: The synthesis of compound 2-(2-formylphenoxy)acetamide was achieved by following an easy procedure in the presence of weak base as reagent. A solution of 2-chloroacetamide (1.52 g, 0.016 mol) was mixed thoroughly with K_2CO_3 (3.39 g, 0.024 mol) solution followed by the addition of salicylaldehyde (1.7 mL, 0.016 mol) dissolved in 30 mL of acetonitrile. This reaction mixture was allowed to stir for 24 h at room temperature. Meanwhile, the progress of the reaction was monitored by the TLC. After the completion of reaction, the reagent K_2CO_3 was removed by simple filtration and the solvent was evaporated under reduced pressure, yielding the desired compound (**Scheme-I**). Further compounds have been studied by many analytical methods such as NMR, FTIR, single crystal XRD and UV-visible spectroscopy.



Scheme-I: Synthetic route of 2-(2-formylphenoxy)acetamide

Crystallization: A simple crystallization technique was used for making the crystal of the synthesized compound. The obtained solid compound (1 g) dissolved in ethanol (30 mL) was warmed at 60 °C in a water bath for 10 min, then filtered to remove the impurities. The filtrate was kept aside to cool

down to room temperature. This study states that the cooling and solvent evaporation processes might help form a crystalline compound. After 10 days, the solvent evaporated completely and a pure colourless crystal was obtained. The trace amount of solvent was further removed by the filter paper and dried at room temperature for 24 h. The obtained pure form of the synthesized compound was further analyzed by single-crystal X-ray diffraction.

Computational studies

DFT studies: For the frontier molecular orbitals (FMO) analysis, compound 2-(2-formylphenoxy)acetamide was optimized by DFT and FMO data were derived from the output file. All the DFT calculations were performed in the Gaussian 09W program software. For the structure optimization of 2-(2-formylphenoxy)acetamide, the B3LYP/6-311++G(d,p) basis set was used and presented in Fig. 1. The experimental bond lengths, bond angles and torsion angles from the X-ray analysis were compared with those obtained with DFT calculations. Table-1 summarizes the experimental and theoretical values of bond length, bond angle and torsion angle. The observed and computed results are quite closely, indicating that theoretical DFT simulations can effectively elucidate the structures of hypothetical substances prior to their synthesis. For the theoretical UV-visible and FTIR experiments, time-dependent DFT and frequency were also calculated and other basic methods were used as well. The Gauss View software was used for various further processes, such as 3D visualization, including FMO, electron cloud identification, molecular electrostatic potential (MEP) and Mulliken charge distribution for the compound FPA.

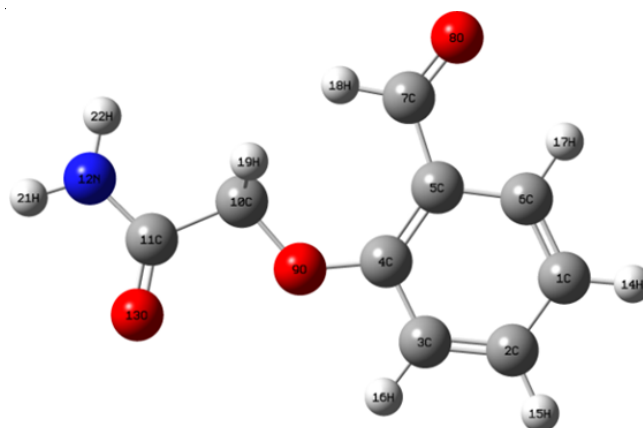


Fig. 1. Optimized structure of 2-(2-formylphenoxy)acetamide molecule

Molecular docking study: In this study, using Auto Dock 4.2, the docking interactions between the 2-(2-formylphenoxy)acetamide and SARS-CoV-2 enzymes were investigated. The protein-ligand complex interaction was visualized using Accelrys Discovery Studio Client 4.1 visualizers. The energetically minimized 3D structure of 2-(2-formylphenoxy)acetamide obtained by single crystal analysis was used for the docking studies. The three-dimensional crystal structure of all the enzymes was taken from the Protein Data Bank. For clarity, bound water and ligand molecules were removed from the enzyme while polar hydrogens were included.

TABLE-1
BOND LENGTHS (Å), BOND ANGLES (°) AND TORSION ANGLES (°) OF 2-(2-FORMYLPHENOXY)ACETAMIDE

Bond length	Exp.	Theor.*	Bond angle	Exp.	Theor.*	Torsion angle	Exp.	Theor.*
N(12)-H(22)	0.85977	1.007	H(22)-N(12)-H(21)	119.938	118.574	C(10)-C(11)-N(12)-H(21)	-179.940	-179.995
N(12)-H(21)	0.86055	1.008	H(22)-N(12)-C(11)	120.090	123.156	C(10)-C(11)-N(12)-H(22)	0.149	0.016
C(11)-O(13)	1.20000	1.209	H(21)-N(12)-C(11)	119.972	118.270	O(13)-C(11)-N(12)-H(21)	-0.122	-0.017
C(11)-N(12)	1.32093	1.368	O(13)-C(11)-N(12)	123.711	123.453	O(13)-C(11)-N(12)-H(22)	179.967	179.995
C(10)-H(20)	0.96983	1.097	O(13)-C(11)-C(10)	125.851	123.758	O(9)-C(10)-C(11)-N(12)	-179.953	-179.976
C(10)-H(19)	0.97039	1.097	N(12)-C(11)-C(10)	110.438	112.789	O(9)-C(10)-C(11)-O(13)	0.234	0.012
C(10)-C(11)	1.50384	1.539	H(20)-C(10)-H(19)	108.442	108.783	H(19)-C(10)-C(11)-N(12)	-59.747	-59.061
O(9)-C(10)	1.40850	1.403	H(20)-C(10)-C(11)	110.171	108.619	H(19)-C(10)-C(11)-O(13)	120.440	120.927
C(7)-H(18)	0.92931	1.098	H(20)-C(10)-O(9)	110.122	111.390	H(20)-C(10)-C(11)-N(12)	59.837	59.104
C(7)-O(8)	1.20700	1.215	H(19)-C(10)-C(11)	110.142	108.617	H(20)-C(10)-C(11)-O(13)	119.967	120.908
C(6)-H(17)	0.92962	1.083	H(19)-C(10)-O(9)	110.133	111.387	C(4)-O(9)-C(10)-C(11)	179.545	179.937
C(5)-C(7)	1.46888	1.484	C(11)-C(10)-O(9)	107.832	107.966	C(4)-O(9)-C(10)-H(19)	59.333	60.892
C(5)-C(6)	1.39016	1.416	C(10)-O(9)-C(4)	117.878	125.761	C(4)-O(9)-C(10)-H(20)	-60.214	-60.761
C(4)-O(9)	1.36260	1.363	H(18)-C(7)-O(8)	118.302	118.414	C(4)-C(5)-C(7)-O(8)	175.358	179.965
C(4)-C(5)	1.40431	1.417	H(18)-C(7)-C(5)	118.182	118.076	C(4)-C(5)-C(7)-H(18)	-4.632	-0.056
C(3)-H(16)	0.92994	1.083	O(8)-C(7)-C(5)	123.516	123.510	C(6)-C(5)-C(7)-O(8)	-6.563	-0.048
C(3)-C(4)	1.39363	1.408	H(17)-C(6)-C(5)	119.634	116.428	C(6)-C(5)-C(7)-H(18)	173.448	179.931
C(2)-H(15)	0.93018	1.084	H(17)-C(6)-C(1)	119.624	120.914	C(4)-C(5)-C(6)-C(1)	-0.709	-0.005
C(2)-C(3)	1.39762	1.380	C(5)-C(6)-C(1)	120.742	122.658	C(4)-C(5)-C(6)-H(17)	179.321	179.998
C(1)-H(14)	0.93078	1.083	C(7)-C(5)-C(6)	119.558	114.979	C(7)-C(5)-C(6)-C(1)	-178.806	-179.983
C(1)-C(6)	1.39102	1.377	C(7)-C(5)-C(4)	120.646	127.416	C(7)-C(5)-C(6)-H(17)	1.224	0.014
C(1)-C(2)	1.38616	1.402	C(6)-C(5)-C(4)	119.769	117.605	C(3)-C(4)-O(9)-C(10)	174.252	179.950
			O(9)-C(4)-C(5)	116.560	129.868	C(5)-C(4)-O(9)-C(10)	-6.088	-0.035
			O(9)-C(4)-C(3)	123.618	110.859	C(3)-C(4)-C(5)-C(6)	1.163	0.005
			C(5)-C(4)-C(3)	119.822	119.272	C(3)-C(4)-C(5)-C(7)	179.238	179.981
			H(16)-C(3)-C(4)	120.372	117.115	O(9)-C(4)-C(5)-C(6)	-179.163	-179.979
			H(16)-C(3)-C(2)	120.361	121.520	O(9)-C(4)-C(5)-C(7)	-1.088	-0.035
			C(4)-C(3)-C(2)	119.313	121.366	C(2)-C(3)-C(4)-C(5)	-0.964	-0.001
			H(15)-C(2)-C(3)	119.408	119.418	C(2)-C(3)-C(4)-O(9)	179.386	179.986
			H(15)-C(2)-C(1)	119.370	120.389	H(16)-C(3)-C(4)-C(5)	179.188	179.994
			C(3)-C(2)-C(1)	121.222	120.193	H(16)-C(3)-C(4)-O(9)	-0.462	-0.007
			H(14)-C(1)-C(6)	120.420	120.464	C(1)-C(2)-C(3)-C(4)	0.317	0.003
			H(14)-C(1)-C(2)	120.456	120.629	C(1)-C(2)-C(3)-H(16)	-179.835	-179.989
			C(6)-C(1)-C(2)	119.124	118.906	H(15)-C(2)-C(3)-C(4)	-179.745	-179.998
						H(15)-C(2)-C(3)-H(16)	0.103	0.010
						C(2)-C(1)-C(6)-C(5)	0.060	0.001
						C(2)-C(1)-C(6)-H(17)	-179.970	-179.997
						H(14)-C(1)-C(6)-C(5)	179.991	179.999
						H(14)-C(1)-C(6)-H(17)	-0.039	-0.002
						C(6)-C(1)-C(2)-C(3)	0.139	0.004
						C(6)-C(1)-C(2)-H(15)	-179.799	-179.997
						H(14)-C(1)-C(2)-C(3)	-179.792	-179.997
						H(14)-C(1)-C(2)-H(15)	0.270	0.002

*Theoretical values were calculated using 6-311++G(d,p) Basis set.

RESULTS AND DISCUSSION

NMR studies: In synthesized compound, 2-(2-formylphenoxy)acetamide, seven protons have been accounted for as characteristic protons, whereas two protons from the amide -NH₂ group have been negligible due to their highly labile nature. The more identical aldehyde proton could be observed in a highly deshielded region and the ether -CH₂ proton could be observed in a shielded region (Fig. 2a). The rest of the four aromatic protons should have appeared in their respective regions. A singlet peak at δ 10.44 ppm is considered a deshielded peak, which corresponds to an aldehyde proton. This confirms the presence of free aldehyde and no more cyclization reaction has occurred. Meanwhile, singlet peaks at δ 4.61 ppm that the

respective two protons get after integration, which is attributed to the ether -CH₂ proton. Three sets of aromatic peaks are observed as doublet, triplet and quintuplet centres at δ 7.73, 7.64 and 7.11 ppm, respectively. The first two peaks show single protons, whereas the last quintuple peak shows two protons after integration. The appearance of the quintuple peak might be a merging of triplet and doublet peaks that each correspond to a single proton. Apart from that, the two broadened singlet peaks observed at δ 7.67 and 7.49 ppm correspond to the amide -NH₂ peak and also show two individual protons for each.

The synthesized compound should have nine peaks in the ¹³C NMR spectrum. Among them, two peaks could appear in a highly deshielded region and one of the carbon peaks should

TABLE-2
COMPARISON OF THE EXPERIMENTAL WAVENUMBERS (cm^{-1}) AND THEORETICAL WAVENUMBERS (cm^{-1}) OF FTIR OF 2-(2-FORMYLPHENOXY)ACETAMIDE CALCULATED BY THE B3LYP/6-311++G(d,p) BASIS SET

Wavenumber (cm^{-1})		Vibrational assignments with PED (%)	Wavenumber (cm^{-1})		Vibrational assignments with PED (%)
Exp. values	Calcd. values		Exp. values	Calcd. values	
3481	3717	sNH(100%)		1040	bHCO(18%), tHCOC(31%), oOCNC(19%)
3402	3589	sNH(100%)		1011	tHCCC(70%)
	3203	sCH(99%)		998	tHCCC(92%)
3155	3199	sCH(88%)		983	tHCCC(81%)
	3188	sCH(92%)		880	tHCCC(82%)
	3173	sCH(91%)		877	sOC(10%), bCCC(13%), bCCC(12%), bCOC(10%), bCCO(14%)
	3038	sCH(50%)		841	sCC(51%)
	3024	sCH(100%)		804	sCC(12%), bOCC(24%), bCCC(10%)
	2988	sCH(100%)	785	780	tHCCC(88%)
1682	1801	sOC(83%)	753	717	tCCCC(16%), tCCCC(27%), tCCCC(25%), oOCCC(11%)
1598	1736	sOC(87%)		652	sNC(10%), bOCN(31%), bCCO(14%)
	1646	sCC(69%)		642	tHNCC(10%), oOCNC(63%)
1578	1624	bHNN(90%)		638	bCCC(11%), bOCC(15%), bCCC(28%), bCCC(11%), bCCC(12%)
	1595	sCC(31%), bCCC(10%), bCCC(15%)		555	sCC(11%), bCCC(10%), bOCC(20%)
	1504	bHCC(18%), bHCC(115%), bHCH(21%)		541	bOCN(32%), bCCC(10%), bCCC(11%), bOCC(14%)
	1495	bHCO(10%), bHCH(53%)		528	tHCCC(11%), tCCCC(26%), oOCCC(31%)
	1474	sCC(13%), bHCC(19%), bHCC(13%), bHCO(17%)		488	tHNCC(60%), bHNCC(20%)
	1450	bHCO(53%)		459	tCCCC(15%), tCCCC(19%), oCCCC(33%)
	1406	bHCH(11%), tHCOC(21%), tHCOC(29%)		415	sCC(14%), bCCC(13%), bOCC(10%), bNCC(32%)
	1366	sCC(16%), sCC(19%), sCC(10%), sOC(19%)		312	bNCC(31%), bOCC(16%)
	1306	sCC(10%), sNC(10%), bHCC(10%), bHCC(12%)		258	bOCC(14%), bCCC(43%), bCCO(13%)
	1286	sNC(22%), bHNC(12%), bHCC(11%), tHCOC(11%)		249	tCCCC(34%), oCCCC(31%), oOCCC(20%)
	1254	bHCO(79%), tHCOC(13%)		214	bOCC(17%), bCCC(23%)
	1248	sCC(19%), sOC(18%), bHCC(10%)		157	tCCCC(19%), tCCOC(26%), oCCCC(12%)
	1203	sCC(11%), sCC(20%), bHCC(31%)		123	tOCCC(16%), tCCCC(17%), tCOCC(36%)
	1178	bHCC(53%)		99	tHNCC(21%)
	1127	sCC(10%), bCCC(10%), bHCC(14%)		96	bCOC(51%), bCCO(27%)
	1108	sOC(37%)		66	tNCCO(12%), tCOCC(11%), tCCOC(49%), oOCCC(11%)
	1076	sNC(25%), bHNC(34%)		55	tOCCC(45%), tCOCC(34%)
	1058	sCC(54%)		28	tNCCO(78%)

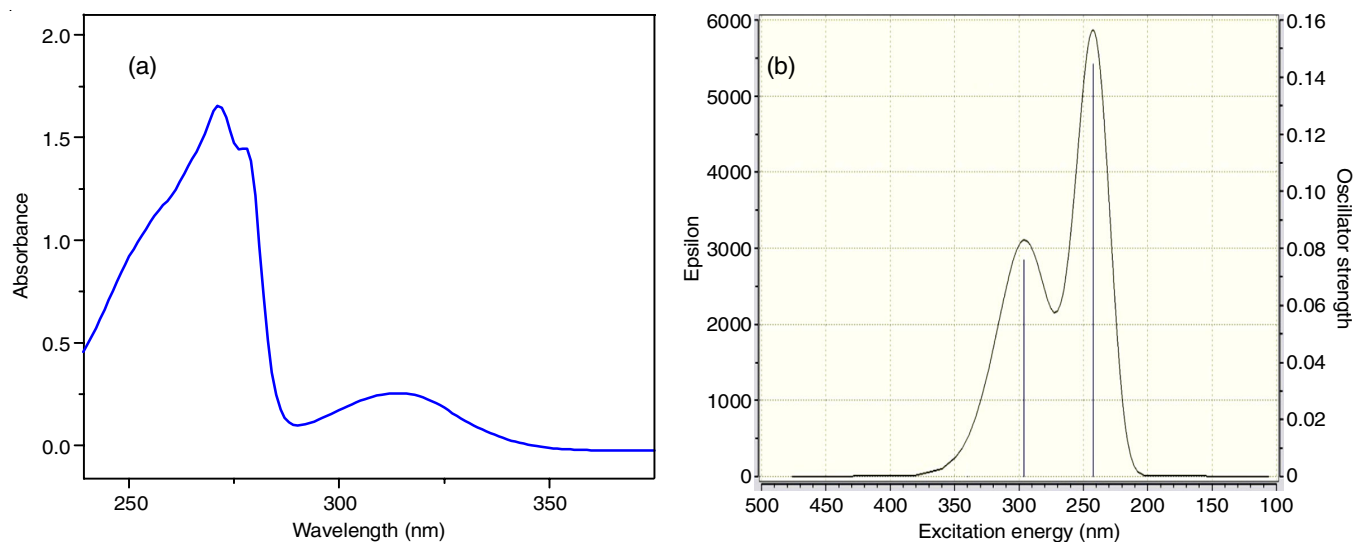


Fig. 4. (a) Experimental and (b) Theoretical UV-visible spectrum of 2-(2-formylphenoxy)acetamide

the experimental data with a small deviation of the wavelength shift towards the blue shift.

Crystal structure determination: The molecular structure of 2-(2-formylphenoxy)acetamide is shown in Fig. 5, with numbering located for all the atoms. The packing diagram of the title molecule shows intermolecular interactions generated by the N–H...O hydrogen bond running down the *a*-axis and the C–H...O hydrogen bond running down the *b*-axis, as shown in Fig. 6. The molecules are oriented in the monoclinic crystal system with a crystalline size of 0.230 mm × 0.270 mm × 0.310 mm. The unit cell parameter is obtained as $a = 8.036(4) \text{ \AA}$, $b = 7.392(3) \text{ \AA}$, $c = 14.196(7) \text{ \AA}$, $\alpha = 90^\circ$, $\beta = 98.260(18)^\circ$, $\gamma = 90^\circ$. The dihedral angle formed between the acetamide and phenoxy rings of the synthesized compound is $6.04^\circ(5)$. The crystal structure reveals that the compound is planar, which is due to the presence of sp^2 carbons, which signifies that all aromatic carbon bond lengths are almost equal. Therefore, the observed double bond character can be inferred by comparing it to the length of the C8–C9 single bond, which measures 1.468 \AA . Both double and single bonds exist between carbon and oxygen, hence indicating the distinct bond lengths. As usual, the single bond of C3–O2 and C2–O2 shows a higher bond length compared to the double-bond carbonyl group. C3–O2 has a shorter bond length ($1.3632 \text{ \AA}(19)$) than C2–O2 ($1.4077 \text{ \AA}(19)$), which is attributed to the hybridization of the carbons. The sp^2 hybridized carbon makes a strong bond with oxygen, whereas the sp^3 hybridized carbon makes a weak bond, leading to a higher bond length. The bond length between O3–C9 is 1.208 \AA , which is equivalent to the double bond character of the carbonyl group. The lowering of the amide carbonyl group has been observed and is also evident in the calculated data. The observed bond length of $1.200 \text{ \AA}(2)$ between O1 and C1 suggests the existence of a resonance structure originating from the lone pair of nitrogen atoms. This resonance contributes to the increased bond strength between oxygen and carbon. Meanwhile, the bond length between N1–C1 is $1.3213 \text{ \AA}(19)$, which also respects the primary amides and confirms that resonance structure. Crystal data, data collection and structure refinement details are summarized in Table-3. The hydrogen-bond geometry for 2-(2-formylphenoxy)acetamide molecule is given in Table-4. This study concluded that title compound has achieved the targeted structure

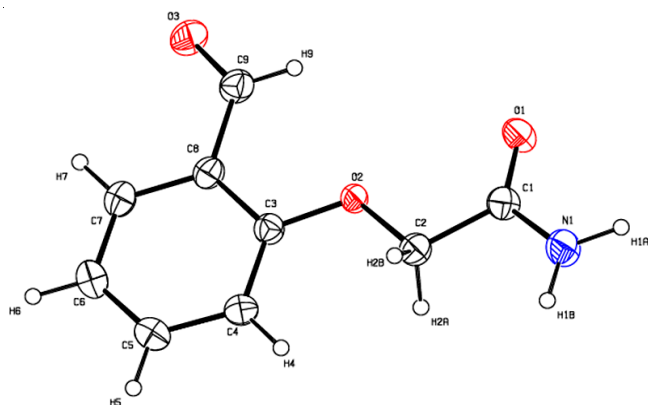


Fig. 5. Molecular structure of 2-(2-formylphenoxy)acetamide showing the atom-labelling scheme. Displacement ellipsoids are drawn at the 50% probability level

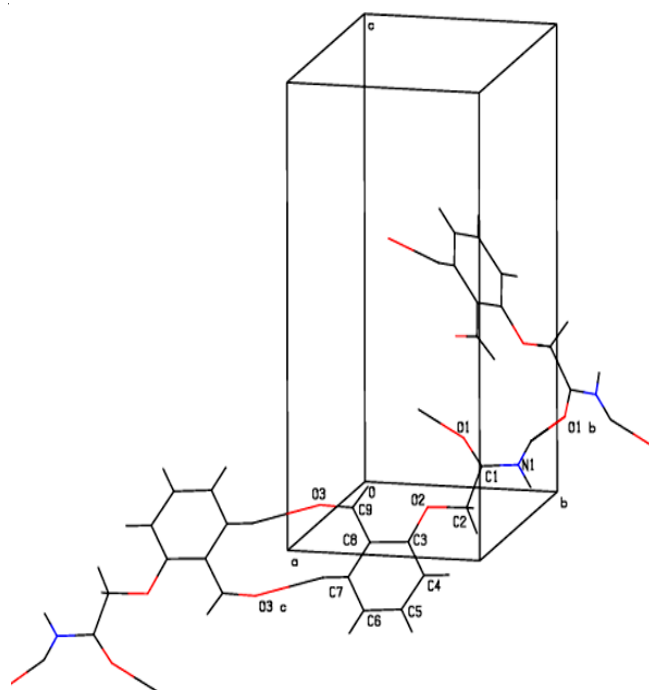


Fig. 6. Packing diagram of 2-(2-formylphenoxy)acetamide showing intermolecular interactions generated by N–H...O hydrogen bond running down the *a*-axis and C–H...O hydrogen bond running down the *b*-axis

TABLE-3
CRYSTAL DATA AND PARAMETERS FOR STRUCTURE
REFINEMENT OF 2-(2-FORMYLPHENOXY)ACETAMIDE

SHELX	
CCDC deposition number	2149564
Crystal data	
Chemical formula	$C_9H_9NO_3$
Mr	179.17
Crystal system, space group	Monoclinic, $P2_1/n$
Temperature (K)	273(2)
<i>a</i> , <i>b</i> , <i>c</i> (Å)	8.036 (4), 7.392 (3), 14.196 (7)
β (°)	98.260 (18)
<i>V</i> (Å ³)	834.6 (6)
<i>Z</i>	4
Radiation type	MoK α
μ (mm ⁻¹)	0.108
Crystal size (mm)	0.31 × 0.27 × 0.23
Data collection	
Diffractometer	Bruker D8 Quest XRD diffractometer
Absorption correction	–
Number of measured, independent and observed [$I > 2\sigma(I)$] reflections	11131, 2421, 1859
R_{int}	0.0699
$(\sin \theta/\lambda)_{max}$ (Å ⁻¹)	0.705
Refinement	
$R[F^2 > 2\sigma(F^2)]$, $wR(F^2)$, S	0.052218, 0.196891, 1.04695
Number of reflections	2421
Number of parameters	121
H-atom treatment	Constr
$\Delta\rho_{max}$, $\Delta\rho_{min}$ (e Å ⁻³)	0.66, -0.49

and confirmed that a highly planar structure might be an essential characteristic for the biomolecule interaction.

TABLE-4
HYDROGEN-BOND GEOMETRY (Å, °) FOR THE
2-(2-FORMYLPHENOXY)ACETAMIDE MOLECULE

D-H...A	D-H	H...A	D...A	D-H...A
N1-H1A...O1 ⁱ	0.93	1.84	2.6956(2)	152
C7-H7...O3 ⁱⁱ	0.93	2.49	3.3886(3)	163

Symmetry codes: (i) 3/2-x, 1/2+y, 1/2-z (ii) 2-x, -y, -z.

DFT studies: This technique allows for the assessment of chemical reactivity, chemical hardness, chemical softness, and the electrophilicity index of the substance. The results revealed that HOMO and LUMO are in the same region where benzene ring behaves as FMO (Fig. 7) and the band gap value was found to be 4.634 eV. The reactivity of the molecules, such as chemical potential, chemical hardness, chemical softness and electrophilicity index, was calculated from the FMO energy values and are given in Table-5. The electrophilicity index has revealed that the compound might show better activity towards biological applications. The following formulae were used to calculate molecule reactivity parameters:

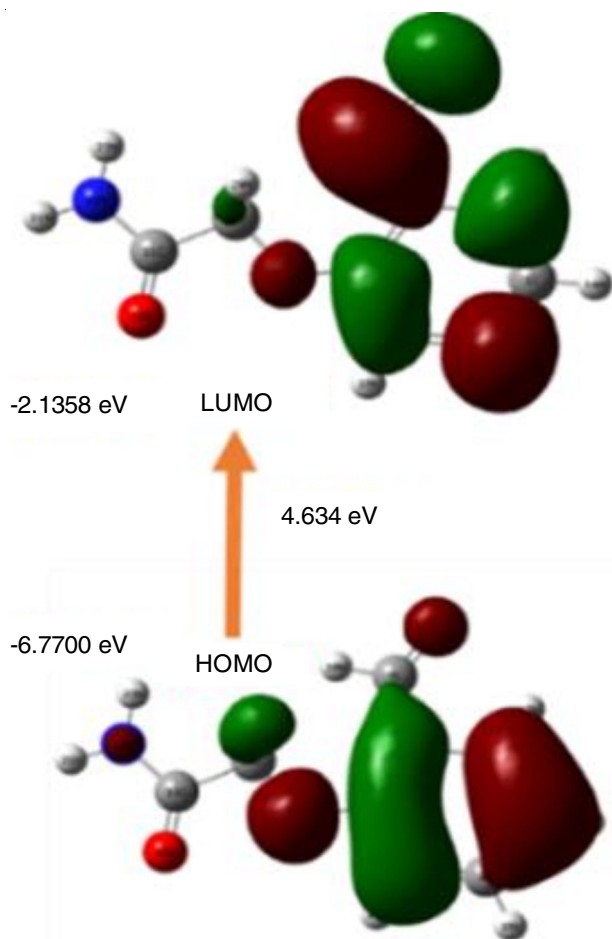


Fig. 7. FMO analysis of the compound 2-(2-formylphenoxy)acetamide derived from the DFT studies

$$\text{Band gap } (\Delta E) = (E_{\text{LUMO}} - E_{\text{HOMO}})$$

$$\text{Chemical potential } 2(\mu) = (E_{\text{LUMO}} + E_{\text{HOMO}})$$

$$\text{Chemical hardness } 2(\eta) = (E_{\text{LUMO}} - E_{\text{HOMO}})$$

$$\text{Chemical softness } (\zeta) = 2\eta$$

$$\text{Electrophilicity index } (\omega) = \mu/2\zeta$$

Molecular docking studies: The title compound was docked with different SARS-CoV-2 virus proteins with the following protein codes: 5R80, 6LU7, 6M0J, 6NUS, 6VSB, 6W9C, and 6YB7. The 3D representation of the docking structure of the studied molecule to the aforementioned proteins are shown in Fig. 8. The detailed parameters such as binding energy, inhibition constant, number of hydrogen bonds and amino acid residues that are involved in the hydrogen bond are presented in Table-6.

Of all proteins, 6NUS has no hydrogen bond, though it shows reasonable binding energy and an inhibition constant value. However, the obtained values are due to the possibility of other interactions, including electrostatic interaction and some weak forces. As a result, the molecule was found to be completely inactive, as evidenced by extremely high values for its binding and inhibition constants.

Two proteins, 5R80 and 6W9C, form a single hydrogen bond with the compound. The ASN203 residue interacts with the 5R80 protein via a carbon-hydrogen bond with a bond length of 3.39 Å. A consistent hydrogen bond was formed between the 6W9C protein and the histidine amino acid residue HIS175, resulting in strong interactions between the two proteins despite the lower bond length of the 6W9C protein compared to the 5R80 protein. This could be replicated in the inhibition constant, which shows a higher constant for the 6W9C (1.35 mM) than the 5R80 (1.03 mM). Meanwhile, the binding constant also appeared to follow the same trend, *i.e.* -4.08 kcal/mol and -3.92 kcal/mol, respectively for 5R80 and 6W9C.

6YB7 protein makes three hydrogen bond interactions with various amino acid residues such as ASN203, GLN110 and PRO293. In Excerpt PRO293, the other two residues involve conventional hydrogen bonds, whereas PRO293 has formed carbon-hydrogen bond interactions. However, the strength of the proline amino acid residue interaction is weaker than the other two. The proline hydrogen bond interaction had a bond length of 3.14 Å while the other two had 2.85 Å and 2.29 Å respectively, for ASN203 and GLN110 residues. The binding constant and inhibition constant for the protein 6YB7 are -4.65 kcal/mol and 389.62 μM, respectively.

Four hydrogen bonding interactions were found in the other three proteins (6LU7, 6M0J and 6VSB). The compound involves four conventional hydrogen bonds with protein 6LU7 *via* three different amino acid residues: ASN151, GLN110 and THR111. Among them, THR111 makes two conventional hydrogen bonding interactions with different bond lengths of

TABLE-5
DFT VALUES OF 2-(2-FORMYLPHENOXY)ACETAMIDE

HOMO (eV)	LUMO (eV)	Band gap (ΔE)	Chemical potential (eV)	Chemical hardness (eV)	Chemical softness (eV ⁻¹)	Electrophilicity index (eV)
-6.7700	-2.1358	4.634	-4.4529	2.3171	0.2157	4.2788

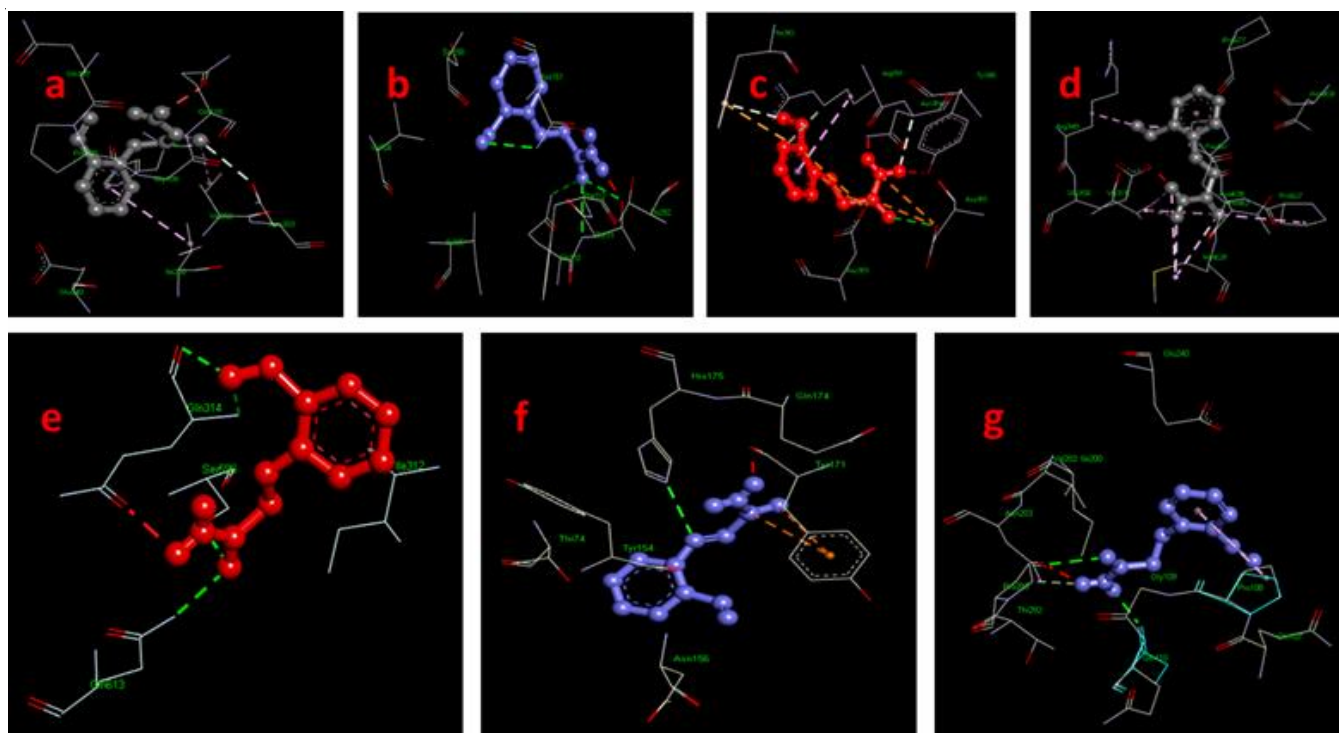


Fig. 8. Molecular docking studies of the compound 2-(2-formylphenoxy)acetamide with various SARS-CoV-2 virus proteins (a) 5R80, (b) 6LU7, (c) 6M0J, (d) 6NUS, (e) 6VSB, (f) 6W9C and (g) 6YB7

TABLE-6
INTERACTION OF DRUG WITH SARS-CoV-2 VIRUS PROTEINS

Protein code	Binding energy (Kcal/mol)	Inhibition constant (μM)	No. of hydrogen bonding	Interacted amino acid residues
6NUS	-6.73	34.98 μM	–	–
5R80	-4.08	1.03 mM	1	ASN203 (3.39 Å) carbon hydrogen bonding interaction
6W9C	-3.92	1.35 mM	1	HIS175 (3.05 Å) conventional hydrogen bonding interaction
6YB7	-4.65	389.62 μM	3	ASN203 (2.85 Å) conventional hydrogen bonding interaction GLN110 (2.29 Å) conventional hydrogen bonding interaction PRO293 (3.41 Å) carbon hydrogen bonding interaction
6LU7	-4.37	623.98 μM	4	ASN151 (3.12 Å) conventional hydrogen bonding interaction GLN110 (2.95 Å) conventional hydrogen bonding interaction THR111 (3.10 Å) conventional hydrogen bonding interaction THR111 (2.95 Å) conventional hydrogen bonding interaction
6M0J	-4.65	391.04 μM	4	ASP382 (3.28 Å) conventional hydrogen bonding interaction ASN394 (3.06 Å) carbon hydrogen bonding interaction AGR393 (3.62 Å) carbon hydrogen bonding interaction PHE390 (3.45 Å) pi-donor hydrogen interaction
6VSB	-3.73	1.83 mM	4	GLN613 (2.91 Å) conventional hydrogen bonding interaction SER569 (2.85 Å) conventional hydrogen bonding interaction GLN314 (2.94 Å) conventional hydrogen bonding interaction GLN314 (2.82 Å) conventional hydrogen bonding interaction

3.10 Å and 2.95 Å. The other two residues also have almost the same bond strength, with a bond length of 3.12 Å and 1.95 Å for ASN151 and GLN110, respectively. Overall, a compound having binding and inhibition constants of -4.37 kcal/mol and 623.98 μM respectively, with protein 6LU7.

Likewise, the title molecule interacts with protein 6M0J via three different kinds of hydrogen bonding with four amino acid residues. ASP382 residue has a conventional hydrogen bonding interaction with a bond length of 3.28 Å. The molecule forms two carbon-hydrogen bonds with amino acid residues ASN394 and AGR393, with bond lengths of 3.06 Å and 3.62

Å, respectively. This indicates that the compound has less interaction affinity with AGR393 than ASN394. Another weak interaction was the pi-donor hydrogen bond interaction, which had a bond length of 3.45 Å with PHE390. The total binding and inhibition constants for the aforementioned four interactions are -4.65 kcal/mol and 391.04 μM , respectively.

At last, there are four amino acid residues involved in the same mode of conventional hydrogen bonding interactions with different binding sites. Each interaction shows a better strength of the bonding compared to other protein molecules, resulting in a shorter bond length between them. These strong inter-

actions lead to a higher binding constant and inhibition constant, respectively, of -3.73 kcal/mol and 1.83 mM. Finally, all the molecular docking studies show better binding interactions with all proteins through various types of hydrogen bonding. Thus, title compound that inhibits this protein activity might become a better drug molecule for very pandemic viruses such as SARS-CoV-2.

Molecular electrostatic potential (MEP): The MEP of the synthesized compound FPA shown in Fig. 9 clearly reveals that the oxygen-spotted area displays a red colour, meaning more negative charges. Furthermore, nitrogen has areas of varying shades of blue and green, which can cause an explosion of positive charges. A strong green colour around the amide NH_2 group thus confirms the resonance structure of the amide functional group. In addition to that the $-\text{CH}_2$ group is green in colour; hence, the whole compound has all neutral, negative and positive regions. Therefore, this compound could interact in a very effective manner randomly.

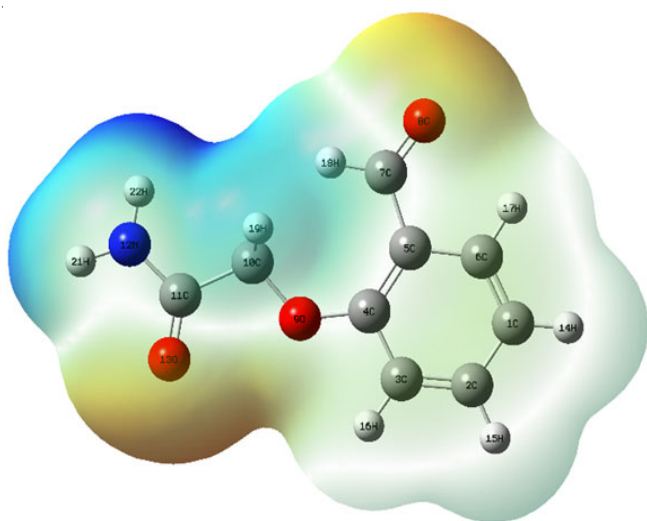


Fig. 9. Molecular electrostatic potential (MEP) mapping of 2-(2-formylphenoxy)acetamide molecule

Mulliken charge distribution: The Mulliken charge distribution of the molecules along with the atomic charge distribution

caused by the atoms present is shown in Fig. 10. The more negative and more positive charges were occupied by the aromatic carbon, which was present in the adjusted position. The carbonyl carbon and oxygen atoms of the aldehyde exhibit a reduced number of negative charges, allowing for more potential interactions with positively charged hydrogen atoms within the biomolecule. Besides, the carbonyl carbon of the amide carbon gets a slightly positive charge, whereas oxygen gets negative charges. At the same time, the nitrogen atom of the amide has a better negative charge than the oxygen due to a more labile lone pair, which is directly involved in resonance. This resonance might reduce the positive charge of the carbon of the amide. The Mulliken atomic charge values of the title molecule are given in Table-7.

TABLE-7
MULLIKEN ATOMIC CHARGES OF 2-(2-FORMYLPHENOXY)ACETAMIDE MOLECULE

Atom	Charge	Atom	Charge
C1	0.043	O2	-0.069
C2	-0.276	O3	-0.246
C3	-1.276	H1A	0.342
C4	-0.374	H1B	0.274
C5	-0.198	H2A	0.202
C6	-0.271	H2AB	0.202
C7	0.196	H4	0.199
C8	1.680	H5	0.179
C9	-0.349	H6	0.164
N1	-0.411	H7	0.209
O1	-0.328	H9	0.138

Conclusion

The synthesized compound 2-(2-formylphenoxy)-acetamide was structurally confirmed by the various spectroscopic analyses and the 3D chemical structure was identified by the single crystal analysis. The results of the crystallographic analysis display the highly planar nature of the title compound. This planar system was significantly influenced by the molecular docking studies, which were performed by the pandemic virus COVID-19 proteins. The studied proteins are more attracted to the synthesized compound, which could be due to

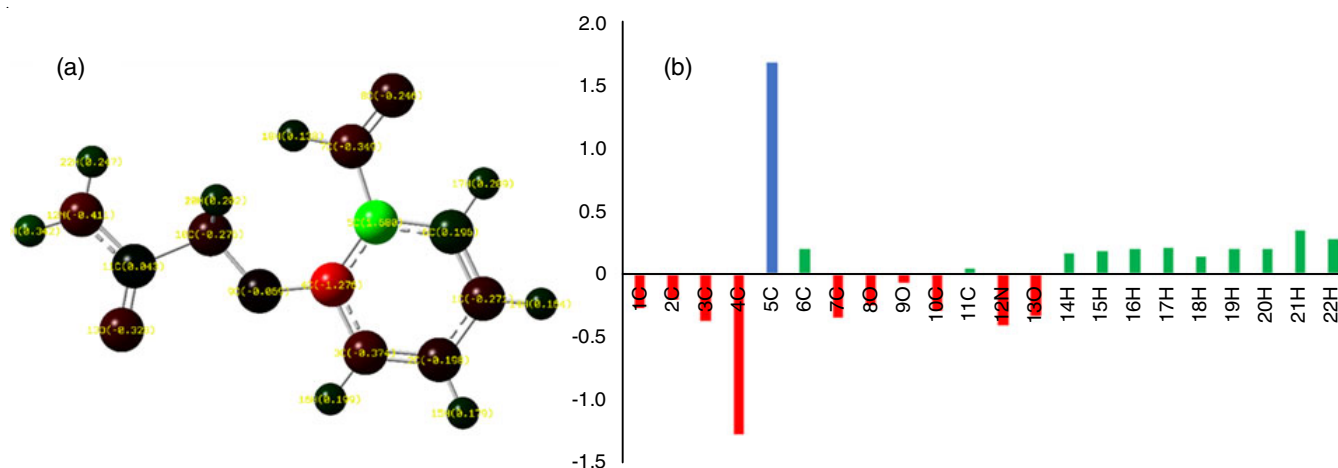


Fig. 10. (a) Mulliken charge distribution of the synthesized molecules, (b) separate atomic charge distribution of the molecule calculated by the Mulliken method

the compound's structural symmetry. The compound shows better binding and inhibition constants with almost all proteins *via* various hydrogen bonding interactions. The obtained results from the other computation methods such as FMO analysis, MEP and Mulliken charge distribution also show linearity with the molecular docking study results. These studies suggested that 2-(2-formylphenoxy)acetamide has a strong binding affinity to COVID-19 proteins and could become a better drug after the detailed evolution of the biological experiments.

CONFLICT OF INTEREST

The authors declare that there is no conflict of interests regarding the publication of this article.

REFERENCES

1. E.B. Denmler and A.S. Frasca, *Can. J. Chem.*, **45**, 697 (1967); <https://doi.org/10.1139/v67-114>
2. G. Jones and B. Abarca, *J. Adv. Heterocycl. Chem.*, **100**, 195 (2010); [https://doi.org/10.1016/S0065-2725\(10\)10007-5](https://doi.org/10.1016/S0065-2725(10)10007-5)
3. N. Kerru, L. Gummidi, S. Maddila, K.K. Gangu and S.B. Jonnalagadda, *Molecules*, **25**, 1909 (2020); <https://doi.org/10.3390/molecules25081909>
4. W.-N. Wu, F.-X. Cheng, L. Yan and N. Tang, *J. Coord. Chem.*, **61**, 2207 (2008); <https://doi.org/10.1080/00958970801901329>
5. W.-N. Wu, Y. Wang, A.-Y. Zhang, R.-Q. Zhao and Q.-F. Wang, *Acta Cryst.*, **E66**, m288 (2010); <https://doi.org/10.1107/S160053681000471X>
6. A. Greenberg, C.M. Breneman and J.F. Liebman, eds., *The Amide Linkage: Structural Significance in Chemistry, Biochemistry and Materials Science*, John Wiley & Sons: New York (1999).
7. J. Thorner, S.D. Emr and J.N. Abelson, *Methods Enzymol.*, **326**, 601 (2000); [https://doi.org/10.1016/S0076-6879\(00\)26041-2](https://doi.org/10.1016/S0076-6879(00)26041-2)
8. C.R. Kemnitz and M.J. Loewen, *J. Am. Chem. Soc.*, **129**, 2521 (2007); <https://doi.org/10.1021/ja0663024>
9. J.I. Mujika, J.M. Mercero and X. Lopez, *J. Am. Chem. Soc.*, **127**, 4445 (2005); <https://doi.org/10.1021/ja044873v>
10. B. Wang and Z. Cao, *Chem. Eur. J.*, **17**, 11919 (2011); <https://doi.org/10.1002/chem.201101274>
11. S. Mahesh, K.-C. Tang and M. Raj, *Molecules*, **23**, 2615 (2018); <https://doi.org/10.3390/molecules23102615>
12. S. Thakral and V. Singh, *Curr. Bioactive Comp.*, **15**, 316 (2019); <https://doi.org/10.2174/1573407214666180614121140>
13. D. Mijin and A. Marinkovic, *Synth. Commun.*, **36**, 193 (2006); <https://doi.org/10.1080/00397910500334421>
14. D.Z. Mijin, M. Prasccevic and S.D. Petrovic, *J. Serb. Chem. Soc.*, **73**, 945 (2008); <https://doi.org/10.2298/JSC0810945M>
15. W.G. Nichols, A.J. Peck Campbell and M. Boeckh, *Clin. Microbiol. Rev.*, **21**, 274 (2008); <https://doi.org/10.1128/CMR.00045-07>
16. Z. Song, Y. Xu, L. Bao, L. Zhang, P. Yu, Y. Qu, H. Zhu, W. Zhao, Y. Han and C. Qin, *Viruses*, **11**, 59 (2019); <https://doi.org/10.3390/v11010059>
17. R.N. Kirchdoerfer and A.B. Ward, *Nat. Commun.*, **10**, 2342 (2019); <https://doi.org/10.1038/s41467-019-10280-3>